Proc. Natl. Acad. Sci. USA
Vol. 83, pp. 8385–8389, November 1986
Neurobiology

Specific modulation of sodium channels in mammalian nerve by monoclonal antibodies

(node of Ranvier/voltage clamp/eel electroplax/action potential/sodium inactivation)

HAMUTAL MEIRI, EFRAT GOREN, HAGAI BERGMANN, IRENE ZEITOUN, YAFFA ROSENTHAL, AND YORAM PALTI

Department of Physiology and Biophysics, Faculty of Medicine, and Rappaport Family Institute for Research in the Medical Sciences, Technion-Israel Institute of Technology, P.O.B. 9697, Haifa 31096, Israel

Communicated by Michael V. L. Bennett, June 18, 1986

ABSTRACT **Monoclonal antibodies (mAbs) were generated against the sodium channels in the intact membrane of the eel electroplax. These antibodies bind to nodes of Ranvier, as indicated by immunofluorescence. When externally applied to rat nerve fibers one of these mAbs blocks impulse conduction. In voltage-clamp experiments, this mAb was found to attenuate sodium current amplitude without affecting the time course. The dose–response curve was very steep and had an ED_{50} of 133 nM. About half of the mAb effect was shown to be due to a shift, in the hyperpolarizing direction, of the steady-state sodium inactivation versus membrane potential curve. The remaining effect was voltage- and time-independent. This mAb had no effect on the potassium or leakage currents. The results indicate that on the external surface of the sodium channel, there are a number of antigenically similar determinants, which are functionally linked to specific elements of the sodium conductance system. These functionally related determinants were preserved through the course of evolution.**

The generation and conduction of nerve and muscle impulses are mediated by specialized membrane macromolecules, the "ion channels" (1–3). The electrical (1–3), chemical (2, 4–8), and structural (3, 6, 9, 10) characterization of these molecules has been the target of numerous studies. Electrophysiological techniques (1–3, 11, 12), initially employed to study excitability, were the first to be used to study ion channels. These methods were followed by pharmacological (4–8, 13), chemical (8, 14), and finally immunological (15–19) probes, which have been employed to further characterize the ion channels.

The potential of immunological approaches increased greatly with the development of the technique for preparation of monoclonal antibodies (mAbs) (20). Initially, mAbs that react with nonfunctional elements of the voltage-dependent sodium channels of the eel electroplax, in solubilized (16–17) and natural (17) membrane states, were described. These antibodies do not react with any part of the sodium channels in mammalian nerve (16–17). Recently, another class of several mAbs, raised against eel electroplax membrane fragments (21), has been shown to modify excitability in mammalian nerve fibers (22).

In this study the voltage-clamp technique (1–3, 23–31) was applied to single nodes of Ranvier of rat sciatic nerve (24) to characterize in detail the interaction of our mAb SC-72-14 with sodium channels.

The main specific effect of the mAb was found to be a shift in the voltage dependence of the steady-state sodium-inactivation parameter (h_∞). An additional effect of the mAb was to reduce sodium conductance (g_{Na}) with little, if any, voltage and time dependence. Since another mAb of our SC series (denoted SC-72-38) was previously found to increase excitability of myoballs or neuroblastoma cells by changing the kinetics of voltage dependence of sodium channel activation (32), we conclude that the sodium channel has a number of distinctly different epitopes that are linked with different functional elements of the channel.

The publication costs of this article were defrayed in part by page charge payment. This article must therefore be hereby marked "*advertisement*" in accordance with 18 U.S.C. §1734 solely to indicate this fact.

MATERIALS AND METHODS

Voltage Clamp. Single myelinated fibers were isolated from the sciatic nerve of albino rats. The fibers were voltage clamped using the modified Nonner apparatus (23) coupled with computer control of command potential pulses and current sampling, described by Binah and Palti (24). The node was externally perfused with Ringer's solution composed of 154 mM NaCl, 5.6 mM KCl, 1.6 mM $CaCl_2$, and 2.3 mM Tris·HCl (pH 7.4). Temperature was held constant at 15 ± 0.5°C.

The axons were cut, in isotonic KCl, 400–700 μm away from the node, and the composition of the internal solution was controlled by diffusion through the cut ends (29). To monitor possible demyelination and deterioration, each node was photographed in the clamp chamber before and after the experiment.

The h_∞ parameter was determined as a function of membrane potential (V_m) by means of pairs of pulses. The first of each pair was a prolonged (30–50 ms) conditioning prepulse (V_{pp}), which was followed by a depolarizing test pulse (V_p) of 65 mV. The h_∞ parameter was defined as the ratio between peak sodium current (I_{Na}) obtained following a given V_{pp} and the maximal I_{Na} obtained at any V_{pp}. Maximal sodium conductance ($\bar{g}_{Na}$) was defined as the maximal g_{Na}, calculated from $I_{Na}/(V_m - V_{Na})$ (where V_{Na} = sodium reversal potential), obtained at any V_p and V_{pp}.

In between pulses, V_m was held at a level (V_H) adjusted to give the h_∞ parameter a value of 0.70–0.75.

The steady-state sodium-activation parameter (m_∞) was derived from $(g_{Na}/\bar{g}_{Na})^{1/3}$. At the end of each experiment the node was destroyed by strong hyperpolarization; the resulting voltage change was taken as the resting value of V_m. The average V_m value in six preparations was −78 ± 5 mV. Membrane currents, which were sampled by 5-μs intervals by a 10-bit analog-to-digital converter, were corrected on-line for amplifier offset and off-line for leakage (24, 29). Leakage conductance was determined from currents generated by hyperpolarizing pulses, assuming that the leakage cur-

Abbreviations: mAb(s), monoclonal antibody(ies); I, current; I_{Na}, sodium current; h, sodium-inactivation parameter; h_∞, steady-state sodium-inactivation parameter; m, sodium-activation parameter; m_∞, steady-state sodium-activation parameter; $\bar{g}_{Na}$, sodium conductance; $\bar{g}_{Na}$, maximal sodium conductance; V, voltage; V_H, holding potential; V_{Na}, sodium reversal potential; V_p, pulse potential; V_{pp}, prepulse potential; V_m, membrane potential; TTX, tetrodotoxin.

rent–voltage (*I–V*) relationship is linear and crosses the voltage axis at the resting potential. Actually, as potassium channels are open at the V_H used (24), potassium currents were subtracted with leakage.

Monitoring of the Compound Action Potential. The compound action potential from desheathed rat sciatic nerves was measured by means of a specially constructed Lucite chamber. The chamber consisted of a covered narrow slit, the width and depth of which were very close to those of the nerve trunk, such that the volume of short-circuiting external medium was minimal and constant during the perfusion of the nerve with different external solutions. The nerve was stimulated by means of one pair of silver/silver-chloride electrodes, and the propagated action potential was recorded by another pair of electrodes connected to a differential amplifier. The action potential was digitally stored and plotted. Measurements were made in Ringer's solution with or without antibodies of different concentrations (22).

Generation of Antibodies. As detailed by Meiri *et al.* (22), we immunized CD_2F_1 mice with membrane fragments (21) from the electroplax of *Electrophorus electricus*. The solution injected contained 0.5 ml comprising 4.3 pmol of tetrodotoxin (TTX)-binding sites per mg of protein mixed at a 1:1 ratio with complete Freund's adjuvant. Two injections were given, 2 weeks apart, into the foot pads of mice. One month later a booster injection was given i.p. without adjuvant to the most stimulated mouse, and after 3 days this mouse was sacrificed and its spleen cells were fused with nonproducing plasmacytoma cells (NS0/1 derived from NS1/1 Ag4.1) (33). Hybrid lines were grown in hypoxanthine/aminopterin/thymidine selective medium (20, 33).

Antibody Propagation. Selected hybridomas were cloned on soft agar. Their immunoglobulins were collected from tissue culture supernatant and from ascitic fluid. The IgG fraction was isolated by precipitation in 40–50% ammonium sulfate and extensive dialysis against phosphate-buffered saline (PBS). The class of the IgG (IgG2b) was determined by the Ouchterlony double-diffusion method or by ELISA. Antibody concentration was determined by ELISA using a standard curve of IgG solutions (Bionetics, Charleston, SC). The molecular weight of the mAb was measured by NaDodSO$_4$/polyacrylamide gel electrophoresis and was found to be M_r 150.

Prior to each electrophysiological experiment, the mAb was diluted in Ringer's solution from a cold (4°C) stock solution of 0.1–10 mg of mAb per ml of PBS.

Screening Procedure. A four-stage screening procedure of the mAb secreted by the hybridoma culture has been described (22). In this study we used mAb SC-72-14, which has the following characteristics. It binds with the same potency to eel electroplax membrane fragments and to rat brain synaptosomal membrane (22). The binding to both membrane preparations is decreased by veratridine and enhanced by scorpion toxin (*Leirus*) but is unaffected by TTX. Moreover, this mAb stains nodes of Ranvier in rat peripheral nerve. The staining is abolished by veratridine but is not affected by acute demyelination. Finally, the mAb blocks the conduction of the action potential of rat sciatic and optic nerves. All of these findings imply that this mAb binds at the external surface of the membrane with an antigenic determinant associated with nerve excitability and toxin binding.

Other mAbs. Two other mAbs were tested in this study: $5D_{10}$ and $5F_3$, a generous gift from J. P. Brockes, Medical Research Council, London. These mAbs were generated against sodium channels that were solubilized from membranes of eel electroplax and then partially purified (16, 17).

Immunofluorescent Staining. Single myelinated nerve fibers isolated from rat sciatic nerve were preincubated for 20 min with PBS supplemented with 3% normal horse serum and 3% normal rabbit serum (PBS-HR) at room temperature (pH 7.4). They were then incubated with 200 μl of one of the following: (*i*) PBS-HR alone (background); (*ii*) mAb $5D_{10}$, mAb $5F_3$, or mAb SC-72-14 (all in PBS-HR); (*iii*) mAb SC-72-14 inactivated either by precipitation by goat anti-mouse IgG or by preincubation with 10–15 sciatic nerve trunks (until the mAb slightly depressed the compound action potential).

After 1 hr of incubation at room temperature with any of the above (a period sufficient to produce the entire electrophysiological effect), the nerves were washed briefly to remove unbound mAb, fixed for 10 min with 3% paraformaldehyde in PBS, washed thoroughly in PBS, and then incubated for 45 min at room temperature with rhodamine-labeled goat anti-mouse IgG. Following an extensive wash, the nerves were refixed for 20 min, washed well in PBS, dried, and finally mounted in 90% glycerol in PBS for observation and photography.

RESULTS

Measurements of Compound Action Potential and Immunofluorescent Labeling. Dose-dependent attenuation of the compound action potential of rat sciatic nerve by mAb SC-72-14 is shown in Fig. 1 (filled circles). This attenuation, which was obtained within 20–40 min of incubation with 440 nM mAb, was completely reversible by 30–60 min of washout (not shown). One milliliter of mAb solution (440 nM), which was shown to depress the compound action potential by 90% (filled circle, Fig. 1 *Inset*), was incubated for 1 hr with 4–10 sciatic nerve trunks of rat. After a 1-hr preincubation period, the mAb concentration was shown by ELISA to be reduced in proportion to the number of nerve trunks used. As a consequence, there was a proportional loss of the mAb effectiveness in depressing the compound action potential

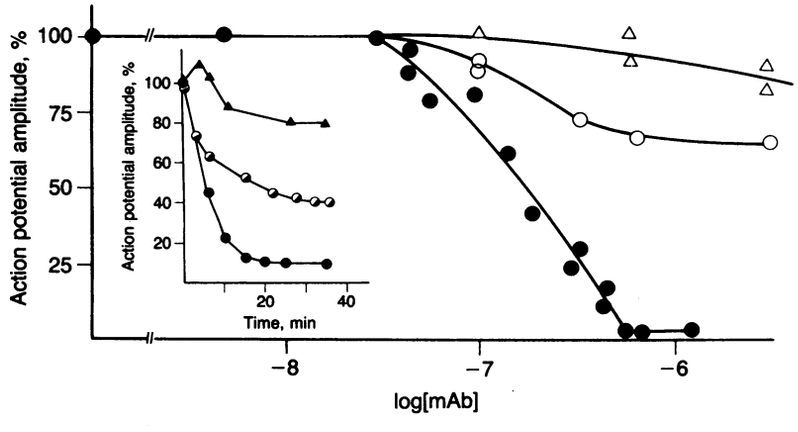

FIG. 1. Dose-dependent depression of compound action potential (%) of rat sciatic nerve. Values were taken after 40–60 min of incubation (a time sufficient to reach steady state) with different concentrations of mAbs: SC-72-14 (●), $5F_3$ (○), $5D_{10}$ (△). (*Inset*) Time-dependent attenuation of compound action potential (%) in rat sciatic nerve. mAb SC-72-14 at 440 nM depressed the compound action potential by 90% within 20 min (●). However, preincubation of 4 sciatic nerve trunks for 1 hr in 1 ml of mAb SC-72-14 (440 nM) reduced the mAb concentration to 180 nM; the mAb depressed the action potential by 60% (◑). Similar preincubation with 10 sciatic nerve trunks reduced mAb concentration to 64 nM; the mAb depressed the compound action potential by 20% (▲). Antibody concentration was determined by ELISA.

(half-filled circles and filled triangles, Fig. 1 *Inset*). These results are consistent with the notion that 10 sciatic nerve trunks contain a sufficient number of sodium channels to bind most of the mAb in 1 ml of 440 nM mAb. Similar treatment of the mAb solution with liver tissue did not modify the effectiveness of the mAb in depressing the compound action potential.

Immunofluorescent staining revealed (Fig. 2*A*) that at an mAb SC-72-14 concentration sufficient to attenuate the action potential by 90%, most nodes of Ranvier were specifically stained (Fig. 2 *A* and *A'*). Moreover, antibodies that lost their blocking power by preincubation with nerve trunks also lost most of their staining potency (Fig. 2 *B* and *B'*). No specific staining was found with the other controls described below (not shown).

Two other anti-sodium channel mAbs, $5D_{10}$ and $5F_3$, which were generated against solubilized and partially purified sodium channels of the eel electroplax (16, 17), were tested in a similar manner. These mAbs, which were shown to be specific to eel sodium channel (1, 16), have no physiological effect in the eel (ref. 34; J. P. Brockes, personal communication). In this study we found that after 1 hr of incubation, mAb $5D_{10}$ reduced the compound action potential by only about 10%, even at concentrations exceeding 850 nM (Fig. 1, open triangles). At this concentration and duration of incubation, we found immunofluorescence staining of <5–10% of the nodes of Ranvier (Fig. 2 *C* and *C'*).

mAb $5F_3$ was a little more potent: at a high concentration of 850 nM, it depressed the action potential by 30–40% (Fig. 1, open circles). This blockage was irreversible. Under these conditions, only 15% of the nodes examined were labeled by this mAb (not shown).

Voltage Clamp. The effect of mAb SC-72-14 on nodal membrane currents is illustrated in Fig. 3. Comparison between the current traces (obtained before leakage subtraction) in Fig. 3 *A* and *B* reveals that the early transient inward (sodium) currents were significantly attenuated by the mAb, whereas the steady-state outward currents, which reflect leakage current and current through a particular class of potassium channels—which are opened at the V_H (24)—remained unaffected. After scaling up the attenuated current

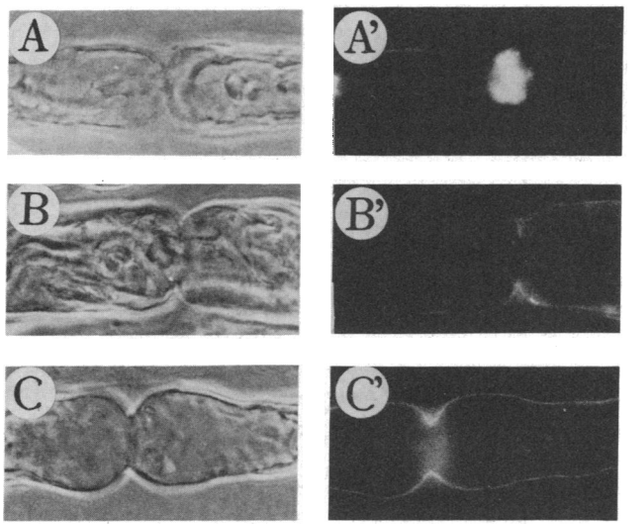

FIG. 2. Immunofluorescent staining of single axons of rat sciatic nerve. The pairs of micrographs represent phase-contrast (*A–C*) and fluorescent (*A'–C'*) images. (*A* and *A'*) Staining with mAb SC-72-14 (66 nM). (*B* and *B'*) Staining with SC-72-14 after preincubation with 10 sciatic nerve trunks for 1 hr (i.e., until the mAb just marginally depressed the compound action potential). (*C* and *C'*) Staining with mAb $5D_{10}$ (1.3 μM). At lower $5D_{10}$ concentration, there was no staining at all. (×550.)

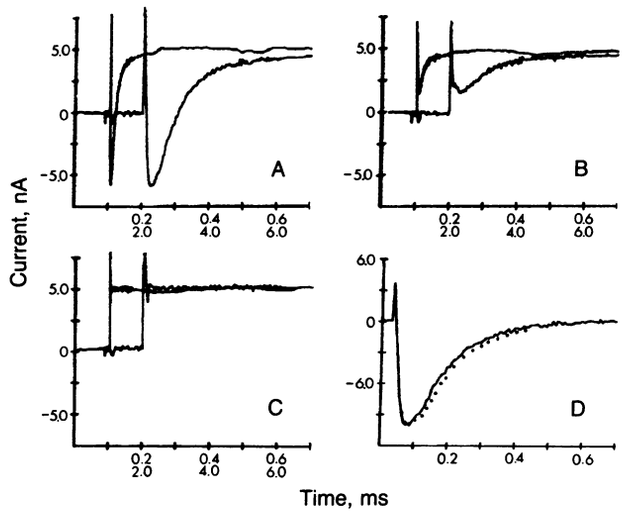

FIG. 3. Computer-reconstructed current tracing obtained during voltage clamp of mammalian (rat) node of Ranvier, illustrating the effects of the antibodies on the transient inward (sodium) currents. Each current was generated by a 30-ms, 60-mV depolarizing pulse. (*A–C*) Each consists of two traces of the same current displayed in two time scales to show the fast transient inward (sodium) current and the steady-state outward current. (*A*) Control current traces in Ringer's solution. (*B*) Current traces of the same node after 20 min of perfusion with 660 nM mAb SC-72-14 in Ringer's solution. The mAb was added while the axon was clamped. (*C*) Current traces recorded in the presence of high external K^+ concentration (56 mM NaCl substituted by KCl) in addition to the antibody at 660 nM. The instantaneous onset of outward current is due to the fact that all potassium channels are open under these conditions (24). (*D*) Current traces obtained in the presence (dots) and absence (continuous curve) of antibody. The currents in the presence of antibody have been scaled up by multiplying each value by 3.54 to illustrate the similarities in time course and shape.

to compare with the control current trace (by multiplying it by a factor of 3.54), the traces became practically identical (Fig. 3*D*). Using a similar procedure for different potentials and utilizing better temporal resolution, it was found that the effects of the mAb on I_{Na} activation and inactivation kinetics were very small (not shown).

The effect of the mAb on peak I_{Na}, as a function of V_m, can be seen in the *I–V* curves depicted in Fig. 4*A*. In the presence of 660 nM mAb, the peak current was attenuated to 24% of the control value (in the absence of mAb). The attenuation was seen to be independent of V_m, and the peak of the *I–V* curves did not shift along the potential axis, indicating that the series resistance error was negligible (35). Fig. 4*B* plots the values of maximal peak I_{Na} obtained from *I–V* curves (see Fig. 4*A*) as a function of mAb concentration (dose–response curve). At a concentration of 200 nM, the maximal peak I_{Na} was only 20% of the control. The apparent ED_{50} was 133 nM. The sigmoidal dose–response curve was very steep—i.e., the I_{Na} attenuation occurred within a small range of mAb concentration (one-third of a logarithm unit).

At a mAb concentration sufficient to depress the maximal peak I_{Na} by 80% (maximal effect), the amplitude of the action potential was much less attenuated. This difference was expected, since an 80–90% reduction in I_{Na} is required to reduce the action potential amplitude by about 50% (2). The nonlinear relationship between I_{Na} attenuation and action potential depression may also account for the difference between the shape of the dose–response curves of Figs. 1 and 4*B*.

The observed effect of mAb SC-72-14 on the g_{Na} system could be analyzed in Hodgkin–Huxley (1) terms as (*i*) changes in the voltage- and time-independent parameter $\bar{g}_{Na}$ and/or (*ii*) changes in the voltage- and time-dependent conductance

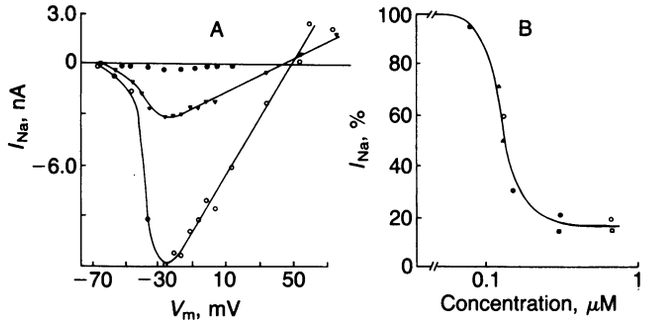

FIG. 4. (A) Values of peak I_{Na} elicited by a series of depolarizing pulses as a function of V_p (I–V curves). ○, Current values obtained during external perfusion with normal Ringer's solution; ▲, current values obtained in Ringer's solution containing 100 μg of mAb SC-72-14 per ml (660 nM); ●, current values obtained at high-potassium Ringer's solution (56 mM NaCl substituted by KCl) in addition to mAb SC-72-14 at 660 nM. The various solutions were added while the axons were clamped at the same V_H. (B) Semilogarithmic plot of the peak I_{Na} values measured from the I–V curve as a function of the logarithm of antibody concentration (dose–response curve). The different symbols represent results obtained from six different axons.

parameters m and h. Fig. 5A illustrates the effect of mAb SC-72-14 on the h_∞ parameter. The general shape and slope of the h_∞ curve was not significantly affected. However, the whole curve was shifted on the voltage axis in the hyperpolarizing direction by 10–15 mV. This shift occurred in the absence of a change in the membrane resting potential as measured in the current clamp. Similar shifts of h_∞ were found in four different experiments. The changes in h_∞ suggest that under a similar set of conditions, the inactivation kinetics might also be modified by the mAb. However, in practice, I_{Na} tracings (such as in Fig. 3B) could not be elicited in the negative membrane potential range where the h_∞ shift could be demonstrated (−120 to −50 mV). Thus, the fact that the current kinetics were not modified (Fig. 3D) does not stand in contrast to the measured changes in h_∞.

At the V_H of about −80 mV, the above changes of the h_∞ parameter could account for only about half of the current (or

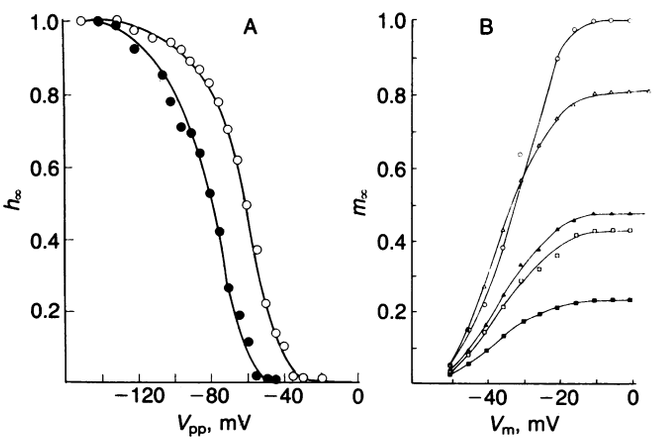

FIG. 5. Antibody interaction with the g_{Na} system. (A) Values of h_∞ as a function of membrane potential. ○, Values obtained in Ringer's solution; ●, values obtained after 10 min of perfusion with mAb SC-72-14 (660 nM). (B) Values of m_∞ versus membrane potential. ○, Control values obtained in Ringer's solution; ▲, values obtained after perfusion with mAb SC-72-14 (52 nM); △, values corrected for the corresponding change of h_∞ obtained at the same mAb concentration; ■, m_∞ values in the presence of 520 nM; □, m_∞ values corrected for the corresponding change of h_∞ obtained at this mAb concentration.

conductance) attenuation (Figs. 3 and 4). Therefore, the effect of mAb SC-72-14 on the m parameter was investigated. To isolate the effect of the mAb on the m_∞ parameter from its effect on the h parameter, all of the measured $\bar{g}_{Na}$ values were multiplied by $1/h_\infty$ at the V_H that compensated for the mAb attenuation of h_∞ (Fig. 5A).

The results of these calculations are seen in Fig. 5B (and were confirmed in three other experiments). It was found that, beyond the effect on h_∞, the mAb significantly reduced g_{Na}. For example, at a mAb concentration that attenuated I_{Na} by 80% (660 nM), m_∞ was reduced by 40% ± 13% (mean of four experiments). However, this attenuation of m_∞ showed little, if any, voltage dependence—i.e., it could be approximately accounted for by a constant factor at all voltages. This additional mAb effect was therefore independent of voltage and time and could therefore be expressed equally well as a reduction of $\bar{g}_{Na}$.

A synergistic effect of high $[K^+]_{out}$ and mAb on the sodium currents is illustrated in Figs. 3C and 4A. Under conditions in which the mAb alone depressed the sodium currents by 75–80% (Figs. 3B and 4 A and B), the currents were practically abolished when 56 mM K^+ (replacing Na^+) was added to the mAb. (The elevation of extracellular potassium concentration did not cause depolarization since the voltage clamp maintained the V_H at the original value of −75 ± 5 mV.) The reduction in sodium currents was approximately twice the measured and predicted attenuation caused by replacing 56 mM Na^+ by K^+ in the absence of mAb (not shown). In fact, the mAb had no effect on the g_{Na} in the absence of potassium ions in the external medium (not shown).

DISCUSSION

This study reveals specific functional modifications of the I_{Na} by mAb SC-72-14 in rat sciatic nerve. The results indicate that some of the channel antigenic determinants, exposed to the external medium, are functionally linked with the g_{Na} system.

Within the Hodgkin–Huxley framework, a change in an ionic current can be attributed to either a change in the ion driving force or a change in the specific channel properties. We showed, using our voltage- and current-clamp protocol, that the mAb does not significantly change the V_m or the V_{Na}. Thus, we can conclude that it does not affect the relevant internal ion concentrations—i.e., the ion driving forces—and that, therefore, its effects must be mediated through the ion conductances.

About half of the conductance attenuation was found to be related to a voltage shift of the inactivation function. The residual reduction of g_{Na} was found to be voltage- and time-independent. Although the effect on inactivation was most likely due to a reduction of the probability of a channel to be in the open state, the residual effect could most probably be attributed to a reduction in the number of the available channels or to a reduction of the individual channel conductance. The distinction between these possible mechanisms cannot be made within macroscopic current measurements and will most likely be resolved by single-channel recordings.

The steepness of the dose–response curve—i.e., the current attenuation versus mAb concentration—is consistent with a multimolecular interaction between the mAb and the sodium channel. This, together with the different functional effects of the mAb, would predict that the sodium channel consists of a number of antigenically similar, but functionally dissimilar, elements. Interestingly, the recent description of the sodium channel sequence of eel electric organ (36) has shown that there is a part of the sequence of the eel channel which is repeated four times. If this repeated sequence (or at

least a part of it), extends four times to the external solution, it could be the molecular basis for multiple sites for our mAb SC-72-14 on a single sodium channel.

The nature of the multimolecular interaction between mAb SC-72-14 and the sodium channel could not be analytically investigated here, either by Hill analysis or by other methods, since the mAb is an IgG capable of monovalent, divalent, and mixed interactions. If the ligand reacted monovalently (as most mAbs do), one could assume the binding of two to seven molecules [40 Å each (37)] per single sodium channel [overall size, 100–300 Å (2)]. If the mAb reacted bivalently (as some mAbs do), only one to three ligand molecules might bind to each channel. However, a bivalent ligand, with about 110 Å separating its sites (37), can cross-link (38) two channels [center-to-center mean distance, about 200 Å (39, 40)]. The actual role of binding can be resolved using data from experiments with Fab fragments.

Our results reinforce previous studies, based on neurotoxins, indicating that sodium-inactivation gating mechanisms are accessible from the external surface of the membrane or that they are allosterically linked with a surface molecule (4–8). Since other agents affect the inactivation system from the internal surface of the membrane (2, 3), it seems that inactivation is accessible from both sides of the membrane.

In view of the fact that all antibodies thus far generated against the solubilized channel do not show functional activity in any preparation (this study as well as refs. 15–19), it seems that the functional elements of the channel are more powerful immunogens in the natural membrane. Indeed, the employment of membrane fragments as an antigen has led to the production of several physiologically active mAbs. For example, mAb SC-72-38 (32), which was generated in the same fusion experiment as SC-72-14, influences the kinetics and the voltage dependency of the m_∞ parameter, whereas mAb SC-72-14 does not. The strongest evidence for a different site is that SC-72-38 is the only mAb that competes with *Tityus* γ toxin in binding to the sodium channel (32). These differences indicate that the two mAbs have two different binding sites on the sodium channel, which are linked to different functional elements of the channel.

Eel electroplax membrane fragments were the antigen for generating the mAb used in this study. However, the mAb was found to interact with sodium channel elements in the phylogenetically distant rat. This cross-reactivity indicates that at least some of the functional elements of the sodium channel have been conserved through vertebrate evolution. These findings are in contrast to the more specific determinants of nonfunctional elements thus far reported (16–18). Therefore, it seems that the sodium channel consists immunologically of at least two types of elements: (*i*) conserved elements, which have functional importance, at least in mammals, and (*ii*) species-specific elements that are modified during the process of evolution.

The antibodies that interact with functional elements of the ion channel provide new tools for studying the chemical structure of functional sites of the sodium channels (36). Using standard immunofluorescence techniques, the antibodies may enable morphological monitoring of channel distribution (15, 22, 40) and estimation of their density. The availability of a large repertoire of antibodies may also be useful in studying differentiation and the development of excitability in cells and tissues (39), under normal (15) as well as a variety of pathophysiological (40) conditions.

We are grateful to Dr. J. P. Brockes, Medical Research Council, London, for his generous gift of mAbs $5F_3$ and $5D_{10}$ and for helpful discussions. We thank Dr. H. Parnas and Dr. A. Levitzki, Hebrew University, Jerusalem, for analysis of the dose–response curve and Dr. M. V. L. Bennett, Albert Einstein College of Medicine, New York, for most helpful comments on this manuscript. In this work, H.M. was supported by Grant 41/81 from the Israel Center for Psychobiology (Charles E. Smith Family Foundation). Y.P. and H.M. were supported by the U.S.–Israel Binational Science Foundation (84-00367) and were recipients of a special grant for neurobiology from the Wolf Foundation. Y.P. was supported by National Institutes of Health Grant 1 RO1 NS17127-01A1. H.M. is a Bat-Sheva de Rothschild Scholar.

1. Hodgkin, A. L. & Huxley, A. F. (1952) *J. Physiol. (London)* **117**, 500–544.
2. Hille, B. (1984) *Ionic Channels of Excitable Membrane* (Sinauer, Sunderland, MA).
3. Armstrong, C. A. (1981) *Physiol. Rev.* **61**, 644–682.
4. Narahashi, T. (1974) *Physiol. Rev.* **54**, 813–889.
5. Cahalan, M. D. (1980) in *Cell Surface and Neuronal Function*, eds. Cotman, C. W., Poste, G. & Nicholson, G. L. (Elsevier/North Holland, Amsterdam), pp. 1–47.
6. Catterall, W. A. (1984) *Science* **223**, 653–661.
7. Levinson, S. R. (1981) in *Molecular Basis of Drug Action*, eds. Singer, T. & Ondarza, R. (Elsevier/North Holland, Amsterdam), pp. 315–331.
8. Lazdunski, M., Balerna, H., Barhanin, J., Chicheportiche, R., Fosset, M., Frelin, C., Poussegur, J., Renaud, J. F., Romey, G., Schartz, H. & Vincent, J. P. (1980) in *Neurochemistry International*, eds. Schoffeniels, E. & Neumann, E. (Pergamon, Oxford), pp. 61–71.
9. Ellisman, M. H., Miller, J. A. & Agnew, W. S. (1983) *J. Cell Biol.* **97**, 1834–1840.
10. Ellisman, M. H., Agnew, W. S., Miller, J. A. & Levinson, S. R. (1982) *Proc. Natl. Acad. Sci. USA* **79**, 4461–4465.
11. Armstrong, C. M. & Bezanila, F. (1973) *Nature (London)* **242**, 459–461.
12. Sigworth, F. J. & Neher, E. (1980) *Nature (London)* **287**, 447–449.
13. Hille, B. (1975) *Biophys. J.* **15**, 615–618.
14. Levinson, S. R. & Ellory, J. C. (1973) *Nature (London) New Biol.* **245**, 122–123.
15. Ellisman, M. H. & Levinson, S. R. (1982) *Proc. Natl. Acad. Sci. USA* **79**, 6707–6711.
16. Moore, H.-P., Fritz, L. C., Raftery, M. A. & Brockes, J. P. (1983) *Proc. Natl. Acad. Sci. USA* **79**, 1673–1677.
17. Fritz, L. C. & Brockes, J. P. (1983) *J. Neurosci.* **3**, 2300–2309.
18. Casadei, J. M., Gordon, R. D., Schotland, D. L. & Barchi, R. L. (1984) *Proc. Natl. Acad. Sci. USA* **81**, 6227–6231.
19. Haimovich, B., Bonilla, E., Casedei, J. M. & Barchi, R. L. (1984) *J. Neurosci.* **4**, 2259–2268.
20. Koheler, G. & Milstein, C. (1975) *Nature (London)* **256**, 495–497.
21. Grunhagen, H. H., Dahl, G. & Reiter, P. (1981) *Biochem. Biophys. Acta* **642**, 267–285.
22. Meiri, H., Zeitoun, I., Grunhagen, H. H., Lev-Ram, V., Eshhar, Z. & Schlessinger, Y. (1984) *Brain Res.* **310**, 168–173.
23. Nonner, W. (1966) *Pflügers Arch. Physiol.* **309**, 116–192.
24. Binah, O. & Palti, Y. (1981) *Nature (London)* **290**, 598–600.
25. Brismar, T. (1980) *J. Physiol. (London)* **298**, 171–184.
26. Chiu, S. Y. (1977) *J. Physiol. (London)* **273**, 573–596.
27. Chiu, S. Y. (1980) *J. Physiol. (London)* **309**, 499–519.
28. Conti, F., Hille, B., Neumcke, B., Nonner, W. & Stampfli, R. (1976) *J. Physiol. (London)* **262**, 729–742.
29. Palti, Y., Gold, R. & Stampfli, R. (1979) *Biophys. J.* **25**, 17–32.
30. Palti, Y., Ganot, G. & Stampfli, R. (1979) *Biophys. J.* **26**, 261–273.
31. Palti, Y., Moran, N. & Stampfli, R. (1980) *Biophys. J.* **32**, 955–966.
32. Barhanin, J., Meiri, H., Romey. G., Pauron, D. & Lazdunski, M. (1985) *Proc. Natl. Acad. Sci. USA* **82**, 1842–1846.
33. Galfree, G. & Milstein, C. (1981) *Methods Enzymol.* **73b**, 1–46.
34. Fritz, L. C. & Brockes, J. P. (1984) in *Neuroimmunology*, eds. Behan, P. & Spreafico, F. (Raven, New York), pp. 23–36.
35. Taylor, R. E., Moore, J. W. & Cole, K. S. (1960) *Biophys. J.* **1**, 161–169.
36. Noda, M., Shimizu, S., Tanabe, T., Takai, T., Kayano, T., Ikeda, T., Takahashi, H., Nakayama, H., Kanaoka, Y., Minamino, N., Kangawa, K., Matsuo, H., Raftery, M. A., Hirose, T., Inayama, S., Hayashida, H., Miyata, T. & Numa, S. (1984) *Nature (London)* **312**, 121–127.
37. Davis, D. R., Padlan, E. A. & Segal, D. M. (1975) *Annu. Rev. Biochem.* **44**, 639–667.
38. Schlessinger, J. & Elson, E. L. (1979) in *Receptors and Recognition*, eds. Cuatrecasas, P. & Greaves, M. F. (Chapman and Hall, London), pp. 78–93.
39. Ritchie, J. M. & Rogart, R. B. (1977) *Rev. Physiol. Biochem. Pharmacol.* **79**, 1–50.
40. Waxman, S. G. & Foster, R. E. (1980) *Brain Res. Rev.* **2**, 205–234.